ON THE ACCURACY OF Cs BEAM PRIMARY FREQUENCY STANDARDS

J-S Boulanger, R.J. Douglas, J. Vanier,
A.G. Mungall, Y.S. Li, C. Jacques

Electrical and Time Standards Section
Physics Division
National Research Council
Ottawa, Ontario, Canada

ABSTRACT

Two effects which influence the accuracy of cesium beam primary frequency standards are examined: (A) second order Doppler shift, and (B) apparent frequency shift upon reversal of the static C-field ($\sim$60 mGauss) in which the hyperfine transitions occur.

(A) A new technique for evaluating the velocity distribution of the Cs beam is presented. Using this method, the second order Doppler shift ($\frac{\Delta f}{f} \simeq 4 \times 10^{-13}$ for our primary standards) can be evaluated to an uncertainty of $\frac{\Delta f}{f} \simeq 10^{-15}$, an improvement on our previous uncertainty of 2×10^{-14}.

(B) Progress in understanding the origins of the frequency shift of our primary standards as the static C-field is reversed in direction is reported. This effect has been eliminated in our evaluations of CsV, but not for the CsVI's.

Application of these methods in evaluating NRC clocks gives no frequency shift outside previously published error budgets.

INTRODUCTION

A major problem with primary cesium clocks is determining the velocity distribution of the Cs atoms, which is necessary to evaluate the second order Doppler shift. Previous approaches either simulated the Ramsey pattern with truncated velocity distributions (Mungall[1]); used the Ramsey pattern itself (Daams[2] and Jarvis[3]); or used pulse excitation (Hellwig[4]). The first two methods suffer from the approximations made either to the form of the velocity distribution or in its calculation from the Ramsey pattern. The third method requires major modification of the microwave excitation system. We haved found another method using the relation between the transition probability at the center of the Ramsey pattern and the (microwave) excitation level. We have shown that this function is a simple

cosine transform of the time of flight distribution. The new method is more accurate and is easier to use than the old methods.

Another problem which was thought to exist in cesium beam clocks is the so-called "Millman effect"[5]. It has been proven by Vanier et al[6] that the Millman effect does not exist for a $\Delta m_F = 0$ transition but only for a $\Delta m_F = \pm 1$ transition. The frequency shift resulting from reversal of the C-field reported earlier by Mungall[5] for CsV, was a consequence of the method used to measure and set the C-field in the normal and reversed field directions (using (4,-4) to (4,-3) transitions). It is not an offset in frequency due to the direction of the C-field. This was demonstrated in CsV, using field dependent transitions with $\Delta m_F = 0$ to measure and set the C-field. However, in the case of CsVI's there is an apparent shift in frequency upon field reversal using either of these two methods.

A - Determination of the velocity distribution

a) The excitation level method
In cesium frequency standards, the transition probability at the resonant frequency of an atom between states p and q is given by[7]:

$$P_{p,q} = 4\sin^2 b\tau \, \cos^2 b\tau, \tag{1}$$

where b is the excitation level and τ the time of flight through one of the two cavities. It can be shown that this relation is true within a part in 10^6 for typical primary cesium standards with currently attainable uniformity of the C-field, microwave excitation level and microwave phase*.

Using simple trigonometric manipulation this equation can be rewritten:

$$P_{p,q} = \frac{1}{2} - \frac{1}{2} \cos 4b\tau . \tag{2}$$

On the other hand, the measured signal amplitude is the integral over all possible times of flight

$$I(b) = \frac{1}{2} \int_o^\infty (1 - \cos 4b\tau)f(\tau)d\tau, \tag{3}$$

which can be rewritten as:

$$I(b) = \text{Constant} - \frac{1}{2} \int_o^\infty f(\tau) \cos 4b\tau \, d\tau . \tag{4}$$

---

* J-S Boulanger, to be published.

The second term is a cosine transform of the time of flight distribution. The reverse operation gives (for $\tau \neq 0$):

$$f(\tau) = \frac{-16}{\pi} \int_0^\infty I(b) \cos 4b\tau \, db \, . \tag{5}$$

Since $v\tau = \ell$, the length of one cavity, it follows that the velocity distribution is:

$$f(v) = \tau^2 f(\tau) \times \text{constant} \tag{6}$$

Consequently it is possible to calculate the time of flight distribution, and hence the velocity distribution, from measurments of the amplitude of the signal at the center of the resonance as function of the excitation level.

Once the velocity distribution is known it can be used in the general Ramsey equation[7] to retrieve the Ramsey pattern of Cs beam intensity vs microwave frequency. This pattern can also be measured and the agreement between the calculated and the measured patterns serves as a check for the accuracy of the velocity distribution. The second order Doppler shift can be evaluated from the velocity distribution in a straightforward manner.

(b) Experimental and computational technique
We used the clocks without modifications although for CsV, the 2-meter clock, we had to change the microwave source in order to obtain sufficient power. These clocks[8] are of the flop-in type with a single cavity providing two excitation regions. The excitation is normally provided by a Gunn oscillator and a calibrated variable attenuator. For the CsVI's, 10 mW of microwave power is available, and the attenuator covers a range of 70 dB. For the present experiment the Gunn oscillator was locked to a separate Cs reference and set at the center frequency of the Ramsey pattern.

The excitation level in the cavity is not known exactly. It can be calculated within a few percent from a knowledge of the cavity Q (loaded $Q \sim 4000$ for our clocks) and the power available. Greater accuracy can be obtained by fitting the calculated Ramsey pattern to the Ramsey pattern measured on the clock. This pattern can be characterized by its shape (the relative amplitude of secondary peaks and valleys to the central peak, the number of peaks, etc.) and by its scale in Hertz (the distance between peaks, or the width at half the height of the central peak, etc).

From the Ramsey equation, it can be seen that, apart from the dependence on b, the shape of the Ramsey pattern is dependent only on the shape of the velocity distribution, if the second order Doppler shifts and the cavity phase differences are neglected (valid for a first approximation). The frequency scale of the Ramsey pattern (or its width) is determined only by the velocity scale (or the average velocity of the distribution), and the clock length.

We adjust a scale factor and recompute the Fourier transform of the excitation level data until the theoretical and experimental widths of the Ramsey patterns are equal. The adjustment is a few percent of the power. This fitting is required once for each clock. The Gunn oscillators are sufficiently stable in power for the same scale factor to be adequate two months after the first measurement, including a reversal of the beam direction.

In order to resolve the Rabi resonances and minimize the effect of the overlapping of the field dependent transitions on the $(3,0)\leftrightarrow(4,0)$ transition at high power levels, the C-field was raised temporarily. As is seen in Figure 1, at 20 dB above the optimum power level for the Ramsey resonance, this effect is quite serious at a C-field of 67 mGauss which is the normal operating field. A magnetic field of 260 mGauss is enough to reduce this problem to acceptable levels as seen in the same figure.

(c) Processing of data
A Fast Fourier Transform (FFT) program was used. It requires data equally spaced in excitation level. Because of the difficulty in satisfying this condition with our attenuator, we used a spline interpolation to extract about 200 points from the 75 experimental points (see Figure 2). We hope in the near future to be able to take more points, improving the accuracy of the data fed to the FFT.

We have also added a "tail" of constant value equal to that of the highest power data point beyond the last measured point to fill the 1024 points needed by the program. This approach is justified by the fact that at high excitation level the detector response tends towards a constant. If the excitation is sufficiently great, even the high velocity atoms make many transitions in passing through the cavities. If we average a large number of atoms at different velocities, the average transition probability is then exactly one half. The effects of adding this "tail" are discussed below.

(d) Effects of experimental difficulties
In order to evaluate the influence of potential sources of error in this method, we have exaggerated four separate error sources and examined the consequences of each. In each case, following the method detailed above, a velocity distribution was obtained, and the scale factor was checked using the widths of the experimental and calculated central Ramsey peaks.

Each time, the quality of the agreement in terms of the shape of the two Ramsey curves could be observed, and changes in the calculated velocity distribution could be noted. For the curves presented in Figures 3 to 6, the agreement between the two Ramsey curves is approximately 1% of the central Ramsey peak. The four sources of errors we have investigated in this manner are:

1) Effect of $m_F \neq 0$ transitions
If the magnetic field is too low, an extraneous signal from neighbouring transitions is added to the true signal for high excitation levels. Comparing Figure 3 with Figure 7-a shows the difference between two sets of data at low (67 mGauss) and high (260 mGauss) magnetic fields. At a low field the effect causes an error at the high velocity end of the spectrum, creating small false velocity peaks. These arise since the signal from the

neighbouring transitions makes I(b) increase as the excitation level is raised. This increase adds peaks in the short time of flight (or high velocity) region.

2) Inadequate microwave excitation level

If the experiment is limited to low values of excitation power, the integral appears to be truncated. The resolution in the time-of-flight distribution is limited, and the velocity distribution is distorted with the addition of an "oscillation" along the velocity axis. The distortion looks much the same as for the first source of error at high velocity and adds some noise at low velocity as can been seen by comparing Figure 4 with Figure 7-a. The peaks at high velocity are due to the offset generated by the "tail" added at the wrong level.

3) Noise in the measured signal

Since the Cs beam noise is much the same at any excitation level, its effect after FFT should be visible in the regions of long times of flight or at low velocities. This effect is simulated in Figure 5 which represents the data of Figure 4 to which a noise equivalent to 5% of the signal maximum has been added before the interpolation. A Ramsey pattern calculated from such a noisy set of data would still give an estimate of the second order Doppler shift within 10 μHz of the noise-free set of data. In practice the noise is below 0.2%.

4) Density of points

As expected, an increase in the density of points gives better results. As can be seen in Figure 6, when compared to Figure 7-c, an increase from 45 to 75 points reduces the noise at low velocities by at least a factor of 4. We expect that doubling the number of points should reduce it even further.

e) Results for each clock: second order Doppler shift

Figures 7-a, 7-b and 7-c show the results obtained on CsVI-A, CsVI-B and CsVI-C respectively. Figures 8-a, 8-b, and 8-c show the Ramsey patterns calculated for each clock from the velocity distribution found by the FFT. For comparison with Figure 8-a, the experimental Ramsey pattern of CsVI-A is also shown in Figure 8. We have suppressed the noise at low velocity, since the geometry of the clock would eliminate all atoms with velocities below a certain value.

It is remarkable how well these curves fit the experimental Ramsey patterns up to a thousand hertz away from the center of resonance (see Figure 8-a). The agreement is better than 1% everywhere. If the deliberately distorted velocity distribution of Figure 3 or Figure 4 is used the agreement is reduced to a region of about 500 Hz around the center of resonance.

Despite this reduction in quality of fit, the second order Doppler shifts, as calculated from these theoretical Ramsey patterns for any one clock, all agree within 10 μHz for a particular clock or one part in 10^{15} of the frequency of the clock. The previous method used for the CsVI's, which assumed a truncated Maxwellian distribution, is in agreement with the present method to within its stated (1σ) error of 2×10^{-14} of the clock frequency.

Unfortunately, the results to date are not as good on CsV. At the time of measurement, the calibrated attenuator used in CsV had a much narrower range (20 dB) than the ones on the CsVI's (70 dB). The use of an uncalibrated attenuator in series with it made the measurements more difficult and the reproducibility was adversely affected. To obtain sufficient microwave power, the Gunn oscillator was temporarily replaced by a 100 mW klystron (also phase locked). The results are shown in Figure 9.

In Figure 9-b the hump at around 150 m/s is false; and, possibly, also the long tail at high velocities (> 500 m/s). A Ramsey pattern calculated from it would be significantly in error. If we used the other sets of data, at low magnetic field or low maximum power, the hump would be displaced and the main peak would also be slightly affected.

Despite that, the Ramsey pattern calculated in Figure 10-b is good to better than 1% up to 500 Hz from the center of resonance. The evaluation of the second order Doppler shift may not be quite as accurate as for the CsVI's. The maximum variation (50 μHz) is 6 parts in 10^{15} of the frequency of the clock using the different sets of data and will likely be improved by using a better attenuator.

It seems that for each NRC clock (CsV and the CsVI's) the second order Doppler shift has been overestimated in the past by the same amount. This error is still within the error limits of the old method that used truncated velocity distributions[1]. Adoption of the new method will reduce the NRC primary clock frequency by 1.7×10^{-14}.

B — The Millman effect revisited

Another source of error in our clocks is the evaluation of the magnetic field needed to operate the clock at zero offset in frequency. It was reported some years ago by A.G. Mungall[5] (1976) that there was a difference in frequency between the two orientations of the magnetic orienting field (C-field) in CsV. An explanation based on the Millman effect was then thought to be the solution, but now proves to be incorrect. A change of method in setting the C-field has eliminated the frequency shift on C-field reversal for CsV.

In the old method, the magnetic field was evaluated with low frequency coils inducing $(4,-4)$ to $(4,-3)$ transitions at 8 points along the beam trajectory. In the new method, the field dependent microwave transitions (m_F = 1 or m_F = -1; Δm_F = 0) are used to evaluate the average field between the exciting cavities. Both methods have been used in the evaluation of the C-field of the four primary Cs clocks in operation at NRC.

For CsV there was typically a fractional frequency shift of 1 x 10^{-13} when the low frequency method was used to set the C-field in the reversed, compared to the normal direction. If the microwave method was used to set the field, no significant shift was observed. The average of the two methods agreed, and since the averaged C-field has always been used for setting CsV, the effect and the change of method for C-field evaluation has had no influence on the CsV time scale. The explanation of the C-field

reversal effect using the old method, in terms of the Millman effect on the clock frequency[5], is wrong. Theoretically, the Millman effect can exist only for $\Delta m_F = \pm 1$ transitions (eg. the old method's low frequency transitions) and not for $\Delta m_F = 0$ transitions (such as the clock transition and the transitions used for the new method)[6]. The results for CsV can be explained completely as a Millman effect acting only on the low frequency transition used for the old method of setting the C-field.

For the CsVI clocks, it was found that the clock frequencies showed frequency shifts with either method for setting the C-field. Furthermore, the frequency determined, using the average of normal and reversed C-field direction, differs for the two methods by up to 1×10^{-13}. The average of normal and reversed C-field determined by the microwave method has always been used for the CsVI clocks, and after evaluation they have agreed with the CsV frequency within a few parts in 10^{14}.
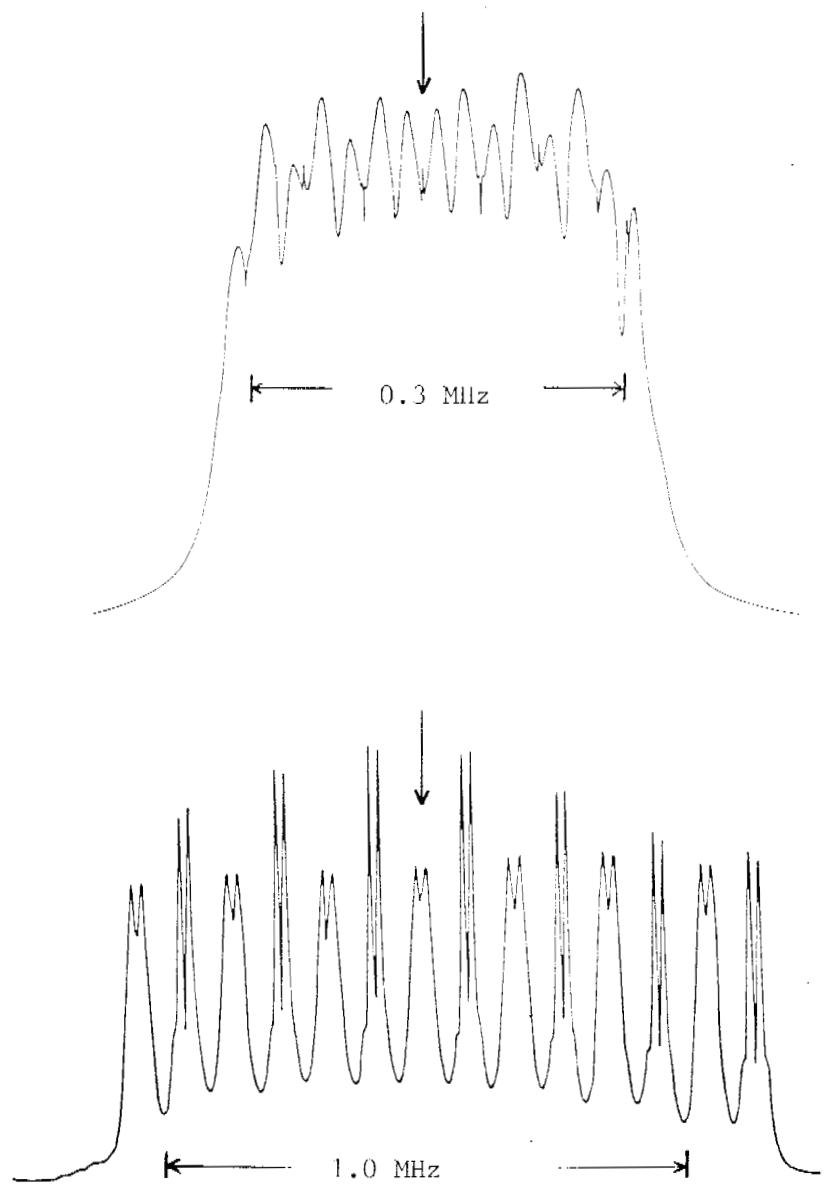
In the case of the CsVI clocks, it seems that the uniformity of the C-field is the source of the problem. In CsV, the magnetic shields are larger than on the CsVI clocks, and any residual magnetic domains affect the uniformity of the field to a lesser extent. Simulating the microwave method, our calculations have shown that if the excitation level is not identical in the two excitation regions, the C-field inhomogeneities (in the excitation regions or in the drift space) can cause Ramsey pattern distortions which make the average frequency differ from the true frequency. Empirically this effect is likely to be small in our clocks since the rates of all four of them are within a few parts in 10^{14} of each other immediately following evaluation.

CONCLUSION
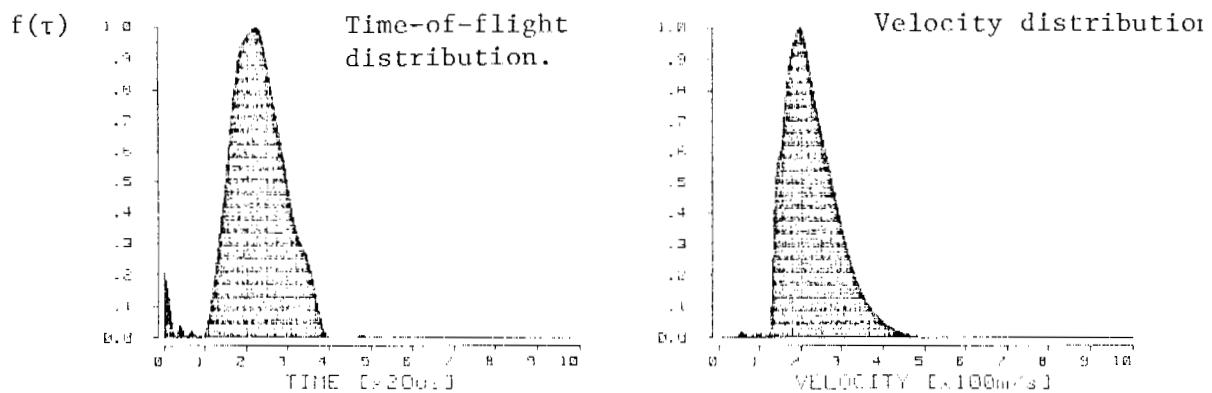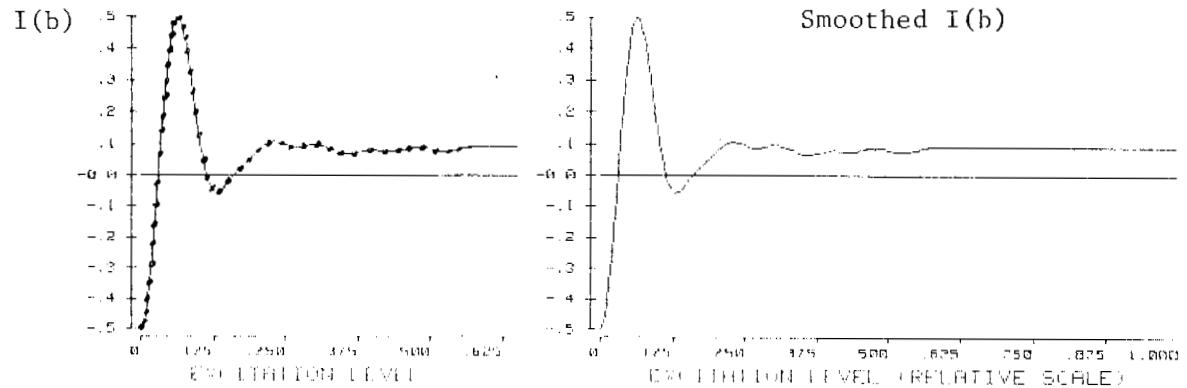
We have presented a new and much more exact method for evaluation of the velocity distribution and the second order Doppler shift in cesium beam frequency standards. This method can evaluate the shift to an accuracy better than a few parts in 10^{15} of the frequency of the clock. It seems feasible to improve the accuracy even further with better measurements. The evaluation of the C-field however is still limited to a few parts in 10^{14} because of the uncertainties linked to the method used, and this uncertainty remains one of the major limitations of NRC's primary clocks.

REFERENCES
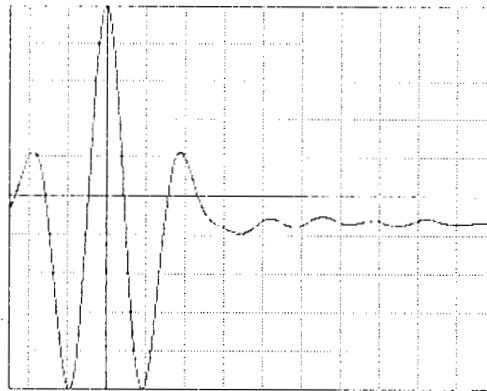
1 A.G. Mungall, "The Second Order Doppler Shift in Cesium Beam Atomic
   Frequency Standards", Metrologia, vol. 7, 49-56, April 1971.

2 H. Daams, "Corrections for Second-Order Doppler Shift and Cavity Phase
   Error in Cesium Atomic Beam Frequency Standards", IEEE Trans. Instrum.
   Meas., vol. IM-23, No. 4, December 1974.

3 S. Jarvis, "Determination of Velocity Distributions in Molecular Beam
   Frequency Standards From Measured Resonance Curves", Metrologia 10,
   87-98, 1974.

4 H. Hellwig, S. Jarvis, Jr., D. Halford and H.E. Bell, "Evaluation and
   Operation of Atomic Beam Tube Frequency Standards Using Time Domain
   Velocity Selection Modulation", Metrologia 9, 107-112, (1973.)

5 A.G. Mungall, "The Millman Effect in Cesium Beam Atomic Frequency
   Standards", Metrologia 12, 151-158, (1976).

6 J. Vanier, A.G. Mungall and J-S Boulanger, "The Millman Effect in Cesium
   Beam Atomic Frequency Standards: Further Considerations", Metrologia 20,
   1984.

7 N. Ramsey, "Molecular Beams", Clarendon Press, Oxford, p. 86 (1956).

8 A.G. Mungall, H. Daams and J-S Boulanger, "Design, Construction and
   Performance of the NRC CsVI Primary Clocks", Metrologia 17, 123-145,
   (1981).

Figure 1. High Power hyperfine resonances as observed in NRC primary cesium clocks. The power level is 20 dB above that for normal clock operation. The seven σ and seven π Rabi pedestals are not resolved at the normal C-field of 67 mGauss (upper curve). At a higher C-field of 260 mGauss the Rabi pedestals are resolved (lower curve), and the $(3,0 \leftrightarrow (4,0)$ Ramsey resonance (vertical arrow) is not greatly contaminated by the neighbouring Rabi pedestals.
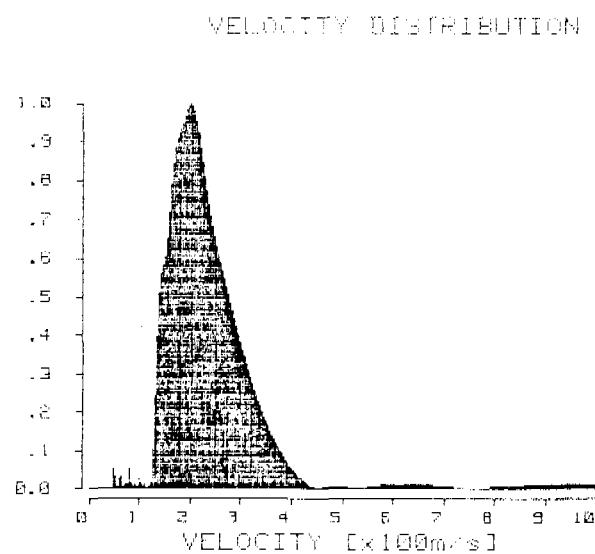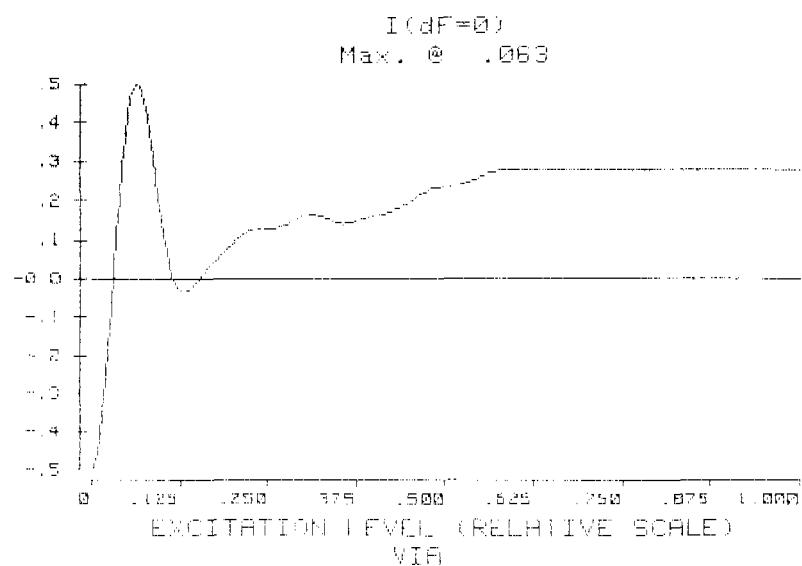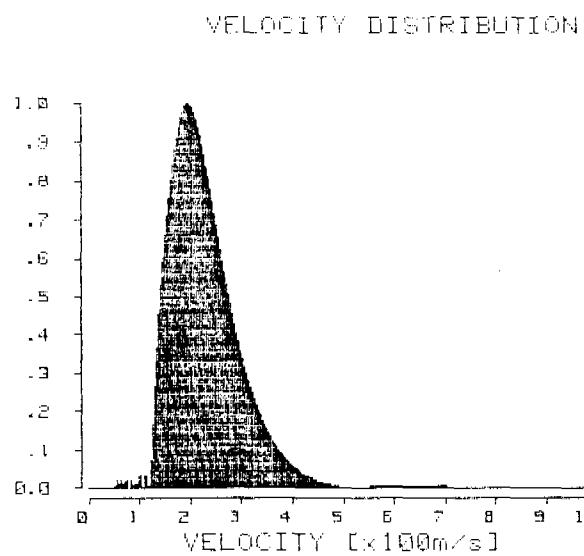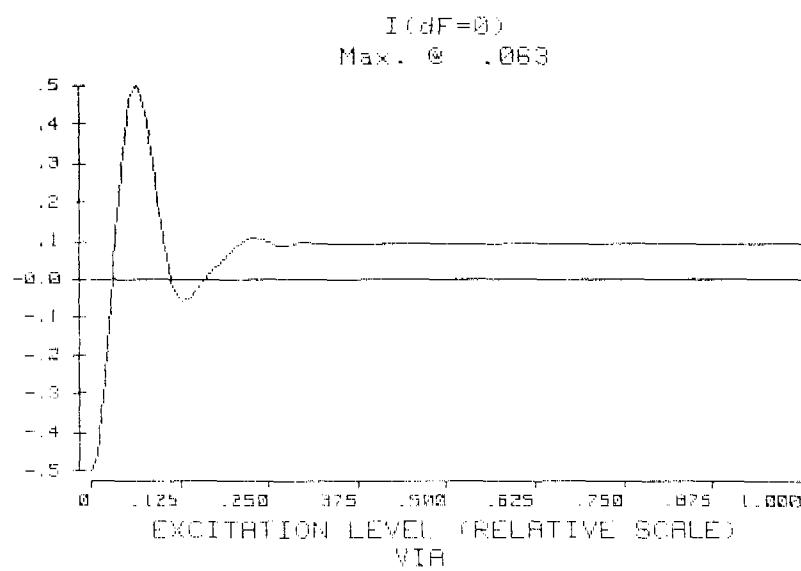
Figure 2. Processing data for CsVI–A.
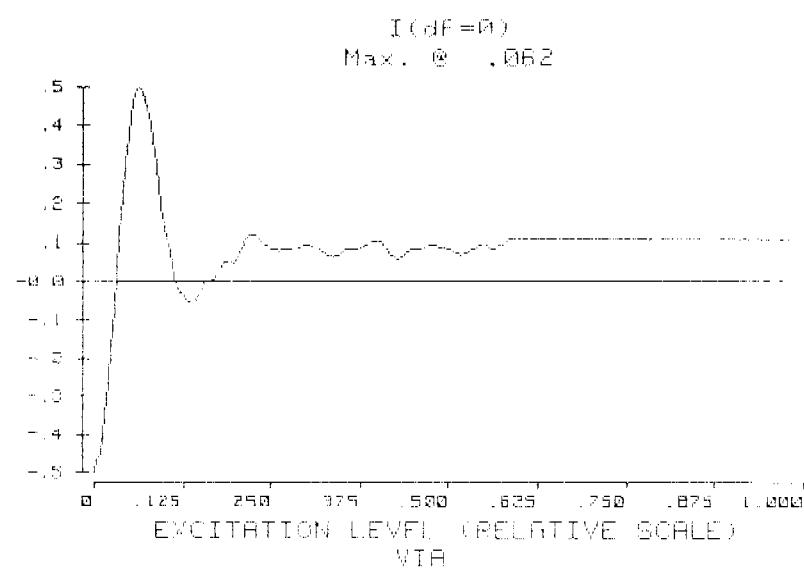
The Cs beam intensity vs (microwave power)$^{\frac{1}{2}}$ at the centre of the $(3,0) \leftrightarrow (4,0)$ Ramsey resonance is the measured I(b) (upper left). Interpolation is used to create a set of equally spaced points, to which a "tail" is added (upper right). This curve is Fourier transformed to obtain the time-of-flight distribution (middle left) through one $\sim$ 1 cm microwave interaction region. The time scale factor is only approximate at this stage. Using $f(\tau)$, the $\sim$ 1 cm distance and Eq. 6, a velocity distribution is obtained (middle right). The velocity scale factor is only approximate at this stage. The scale factor is accurately determined by fitting the width of the calculated Ramsey pattern (bottom) to experiment: this width depends on the mean time of flight between the two interaction regions (2.090 m for CsV, 1.006 m for the CsVI's).
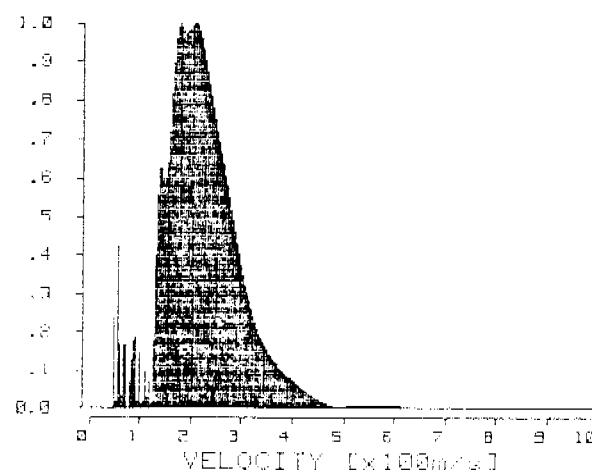
Figure 3.   I(b) (after interpolation) and the velocity distribution determined for CsVI-A at low C-field (67 mGauss). Compared with Figure 7-a, neighbouring transitions have changed I(b), yet the mean velocity (over the range 118 m/s to 457 m/s) is 230 m/s, and the second order Doppler shift for the clock is -23.2×10^{-14} of the clock frequency, vs -23.1×10^{-14} for Figure 7-a.

I(dF=0)
Max. @ .063

EXCITATION LEVEL (RELATIVE SCALE)
VIA

VELOCITY DISTRIBUTION

VELOCITY [x100m/s]
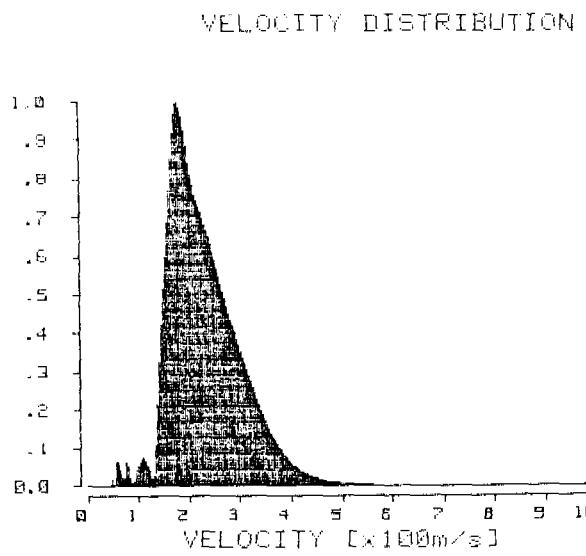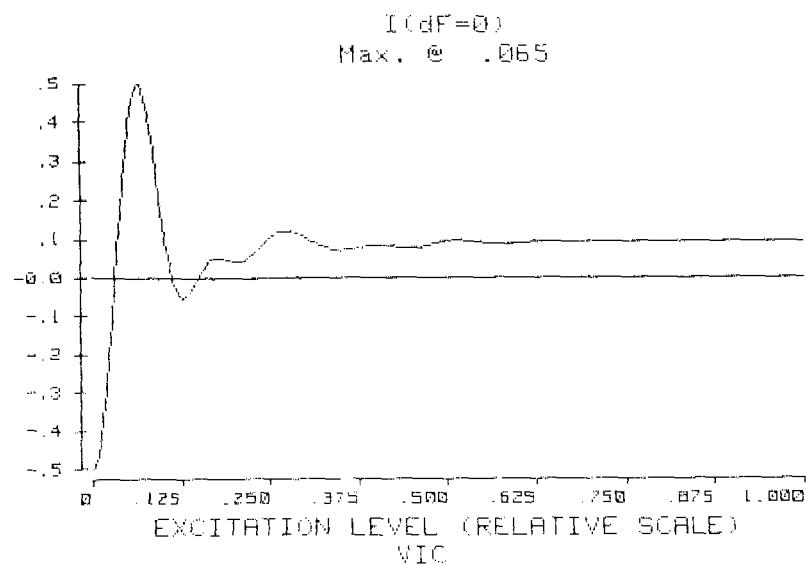
Figure 4. I(b) (after interpolation) and the velocity distribution determined at low maximum microwave power (3 mW) for CsVI-A. Compared with Figure 7-a, in the velocity distribution (10 mW maximum power) there are changes in the velocity distribution (lower resolution and "oscillations"), yet the mean velocity (over the range 121 m/s to 522 m/s) is 230 m/s, and the second order Doppler shift for the clock is -23.1 x 10^{-14} of the clock frequency, vs -23.1 x 10^{-14} for Figure 7-a.

70

I(df=0)
Max. @ .062

EXCITATION LEVEL (RELATIVE SCALE)
VIA

VELOCITY DISTRIBUTION

VELOCITY [x100m/s]
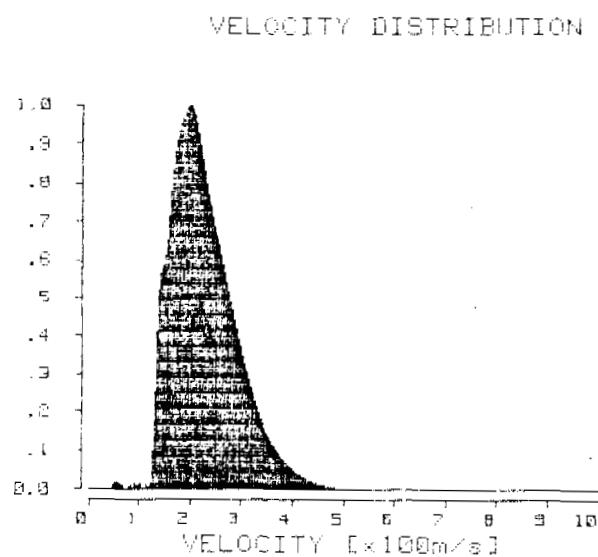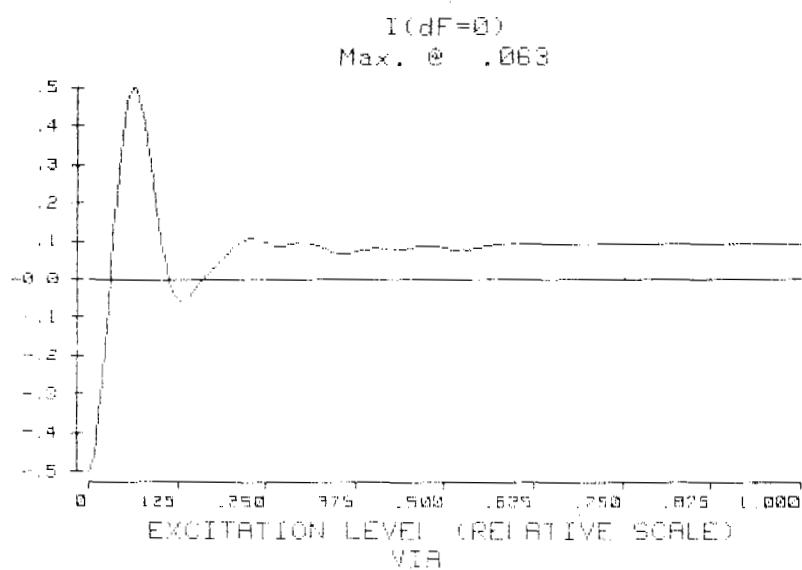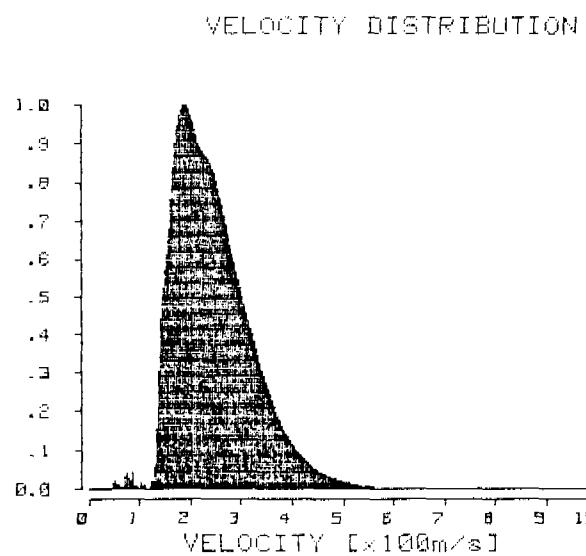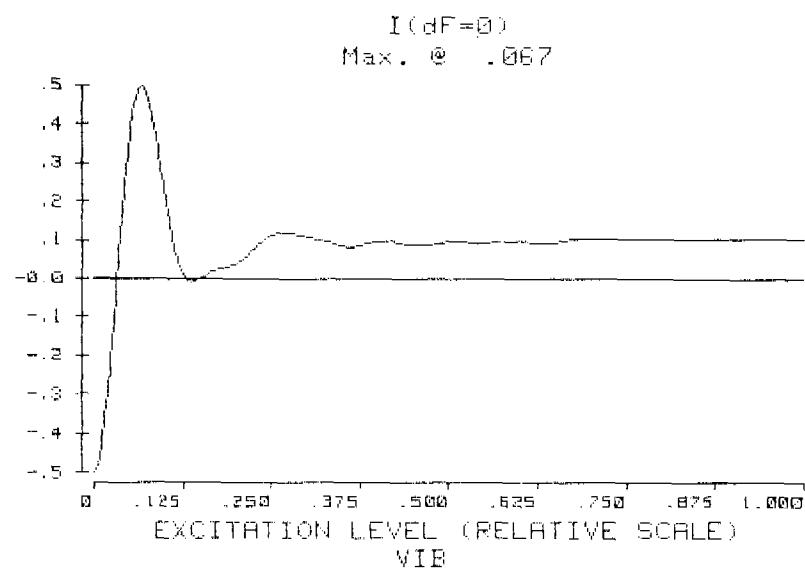
Figure 5.   I(b) (after interpolation) and the velocity distribution
determined for CsVI-A with excess noise added (rms noise is 5% of the
maximum).   This should be compared to Figure 7-A.   The mean velocity (over
the range 122 m/s to 984 m/s) is 232 m/s, and the second Doppler shift for
the clock is -23.1×10^{-14} of the clock frequency, vs -23.1×10^{-14} for
Figure 7-a.

I(dF=0)
Max. @ .065

EXCITATION LEVEL (RELATIVE SCALE)
VIC

VELOCITY DISTRIBUTION

VELOCITY [x100m/s]
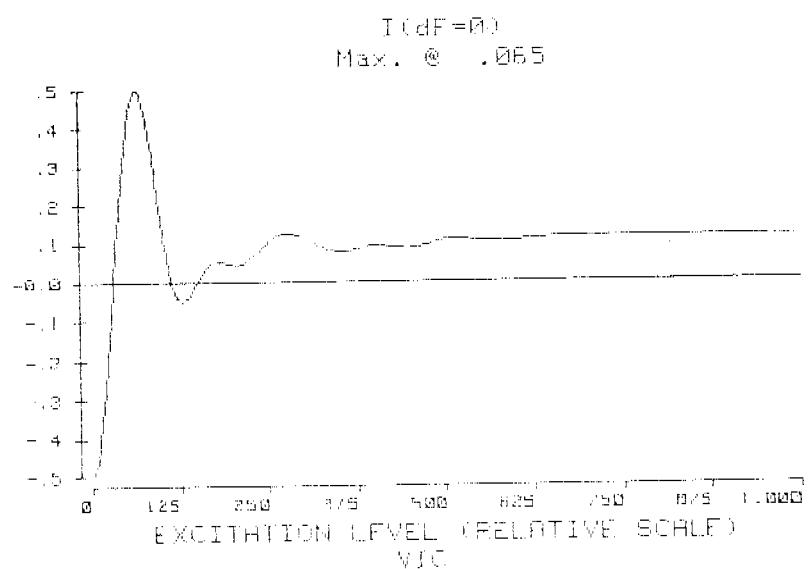
Figure 6. I(b) (after interpolation) and the velocity distribution determined using 45 points of data for CsVI-C. This should be compared to Figure 7-c for which 75 data points were used. The mean velocity (over the range 131 m/s to 700 m/s) is 238 m/s, and the second order Doppler shift for the clock is -24.1×10^{-14} of the clock frequency vs -24.1×10^{-14} for Figure 7-c.

72

I(dF=0)
Max. @ .063

EXCITATION LEVEL (RELATIVE SCALE)
VIA

VELOCITY DISTRIBUTION


VELOCITY [×100m/s]
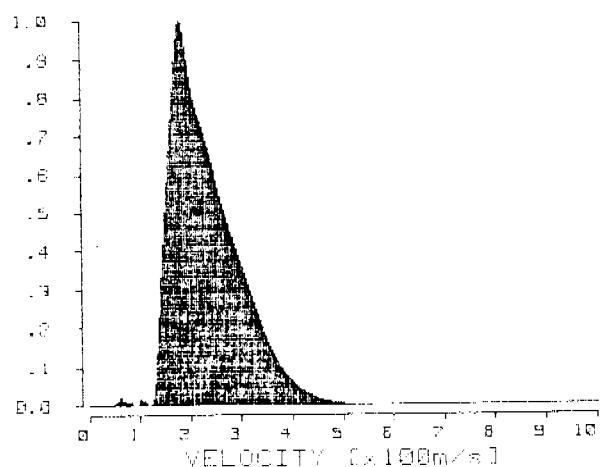
Figure 7-a. I(b) (after interpolation) and the velocity distribution for CsVI-A. The mean velocity (over the range 113 m/s to 522 m/s) is 230 m/s, and the second order Doppler shift for the clock is -23.1×10^{-14} of the clock frequency.

73

I(dF=0)
Max. @ .067

.5
.4
.3
.2
.1
-0.0
-.1
-.2
-.3
-.4
-.5

0   .125   .250   .375   .500   .625   .750   .875 1.000

EXCITATION LEVEL (RELATIVE SCALE)
VIB

VELOCITY DISTRIBUTION

1.0
.9
.8
.7
.6
.5
.4
.3
.2
.1
0.0

0   1   2   3   4   5   6   7   8   9   10

VELOCITY [x100m/s]
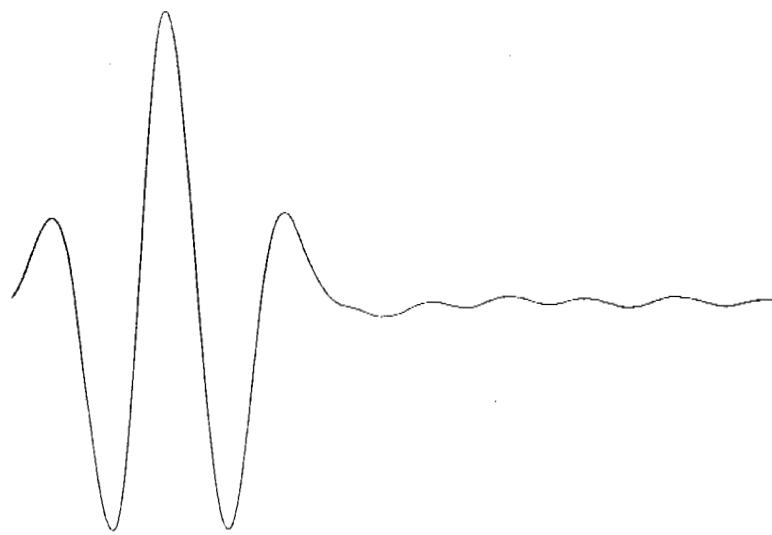
Figure 7-b. I(b) (after interpolation) and the velocity distribution for CsVI-B. The mean velocity (over the range 121 m/s to 610 m/s) is 248 m/s, and the second order Doppler shift for the clock is -25.7×10^{-14} of the clock frequency.

74

I(dF=0)

Max. @ .065


VELOCITY DISTRIBUTION

VELOCITY [x100m/s]
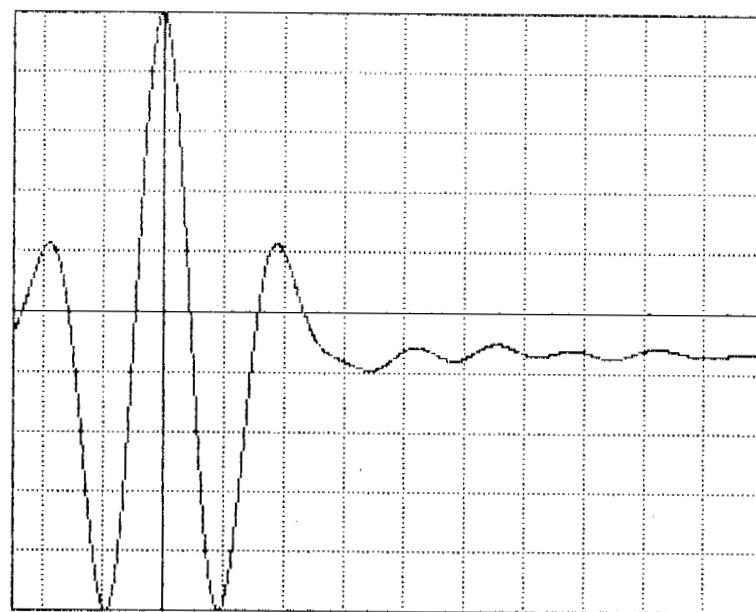
Figure 7-c. I(b) (after interpolation) and the velocity distribution for CsVI-C. The mean velocity over the range 123 m/s to 552 m/s is 236 m/s, and the second order Doppler shift of the clock is -24.1×10^{-14} of the clock frequency.
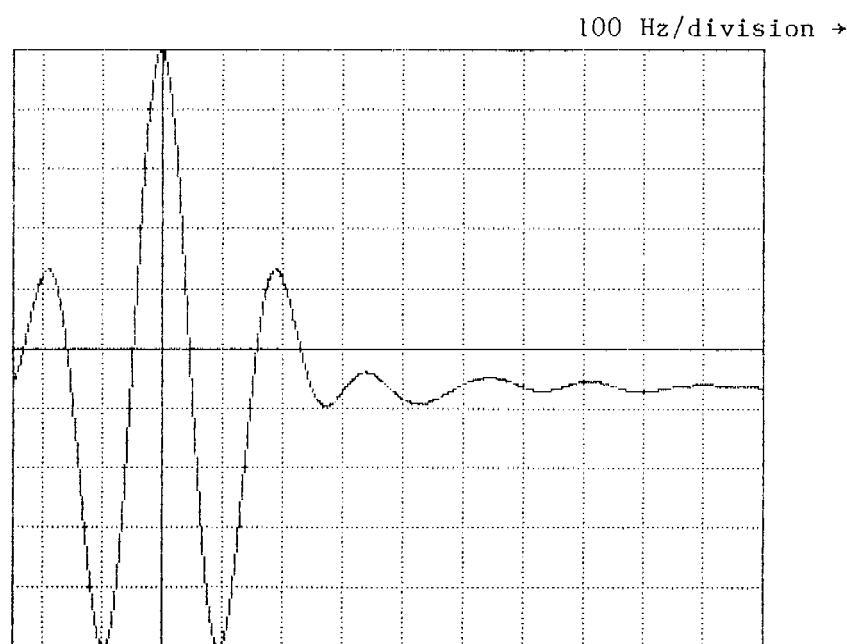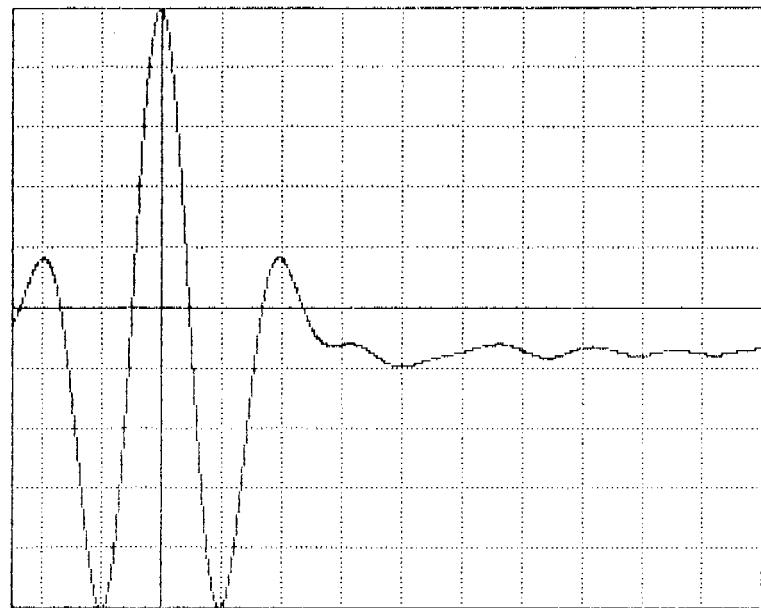
100 Hz/division →
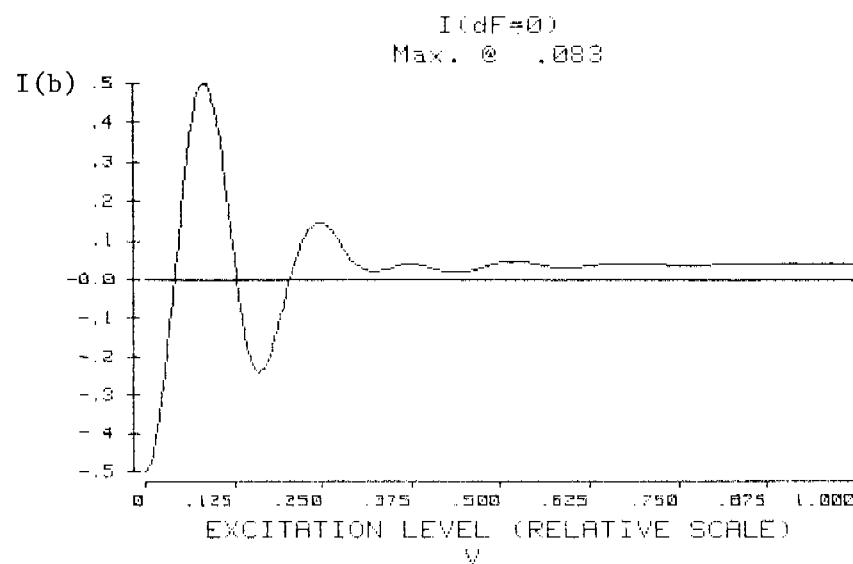
Figure 8-a. Upper: Experimental Ramsey pattern for CsVI-A.

Lower: Calculated Ramsey pattern for CsVI-A.

100 Hz/division →
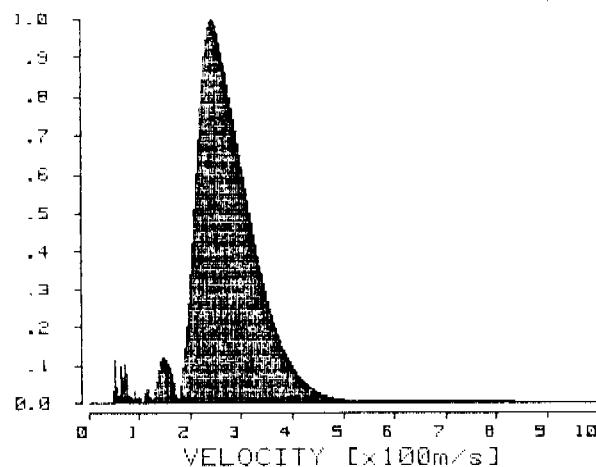
Figure 8-b. Calculated Ramsey pattern for CsVI-B. It differs by less than 1% from the experimental pattern.

Figure 8-c. Calculated Ramsey pattern for CsVI-C. It differs by less than 1% from the experimental pattern.

I(dF≠0)
Max. @ .083

I(b) .5
.4
.3
.2
.1
-0.0
-.1
-.2
-.3
-.4
-.5

0   .125   .250   .375   .500   .625   .750   .875 1.000

EXCITATION LEVEL (RELATIVE SCALE)
V

VELOCITY DISTRIBUTION

1.0
.9
.8
.7
.6
.5
.4
.3
.2
.1
0.0

0   1   2   3   4   5   6   7   8   9   10

VELOCITY [x100m/s]
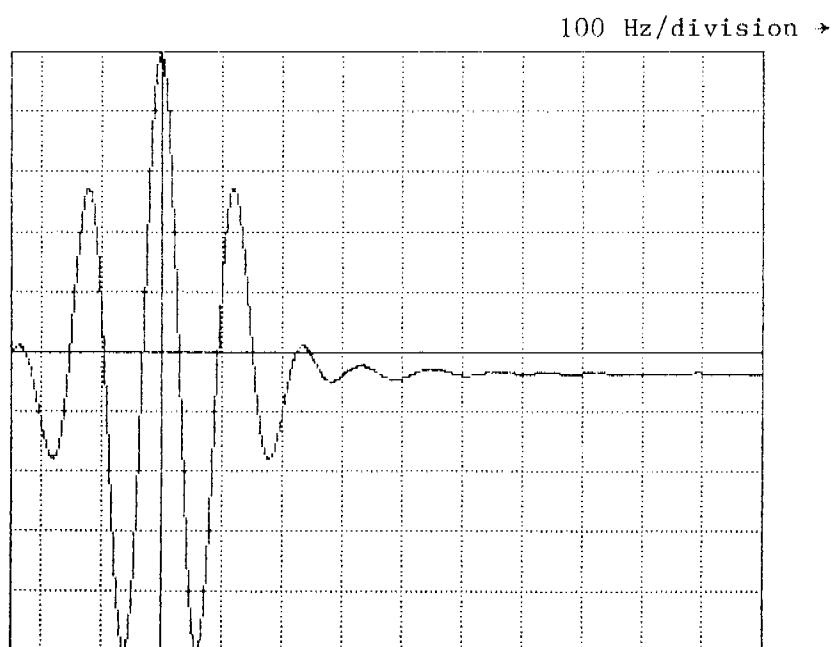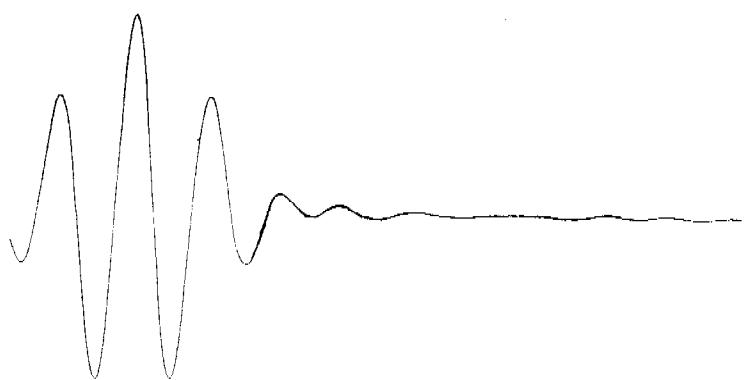
Figure 9-a. Upper: I(b) (after interpolation) for CsV.
The maximum power level is 28 mW. Three sections of I(b) have been matched
to extend the 20dB range of the calibrated attenuator in CsV.

Figure 9-b. Lower: The volocity distribution determined for CsV. The
mean velocity (over the range 178 m/s to 700 m/s) is 283 m/s, and the second
order Doppler shift for the clock is -39.5×10^{-14} for the clock frequency.

100 Hz/division →

Figure 10-a. Experimental Ramsey pattern for CsV.

Figure 10-b. Calculated Ramsey pattern for CsV. It differs by less than 1% from the experimental pattern above.

QUESTIONS AND ANSWERS

DAVID ALLAN, NATIONAL BUREAU OF STANDARDS: The accuracy numbers you quote, are they one sigma, or two sigma, or three sigma numbers?

MR. JACQUES: They are one sigma.

MR. HELLWIG: What is the N. R. C.'s official claim for the realization of the second?

MR. JACQUES: We think that we can safely claim a part in ten to the thirteenth, because, despite all of the problems that we have in the magnetic shields, the frequencies are within one to two parts in ten to the fourteenth, one from the other. But on the other hand, we are not sure how long we can go. Because of those problems in the magnetic shields, we can't evaluate them as well as we would like. We have only Cesium V for which the magnetic shields are very stable. This leaves us with only one clock, which we can't compare to itself.

MR. HELLWIG: You cannot compare using GPS?

MR. JACQUES: We just got the GPS receiver, but the problem is that we need to do these comparisons within twenty-four hours, or possibly forty-eight hours to be sure that they are accurate, especially for the reversal of the beam, which we have to do as fast as possible.